X-646-72-190
PREPRINT

DISTRIBUTIONS AND CHARACTERISTICS OF HIGH-LATITUDE FIELD-ALIGNED ELECTRON PRECIPITATION

F. W. BERKO

JUNE 1972

GSFC — GODDARD SPACE FLIGHT CENTER
GREENBELT, MARYLAND

DISTRIBUTIONS AND CHARACTERISTICS OF HIGH-LATITUDE FIELD-ALIGNED ELECTRON PRECIPITATION

By

F. W. Berko

NASA-Goddard Space Flight Center
Greenbelt, Maryland 20771

JUNE 1972

ABSTRACT

Satellite measurements of field-aligned auroral electron precipitation have been analyzed using 16 months of data from the OGO-4 Auroral Particles Experiment. As seen from the moving satellite, the anisotropies are of short time duration and are most likely to occur when particle fluxes are high. Field-aligned 2.3 keV electron precipitation is found in an oval shaped region primarily in the nighttime hours, with a maximum probability at $\sim 70^{o}$ invariant latitude near midnight, congruent to and poleward of the auroral optical emissions in these hours. This precipitation is found to be associated with the high latitude boundary of auroral electron precipitation during substorm expansion and is characterized by a harder and more intense energy spectrum than typical isotropic precipitation.

INTRODUCTION

Satellite observations of electrons at high latitudes with pitch angle distributions peaked near small values have been reported by several authors. Hoffman and Evans (1968) reported near 0^{o} peaked fluxes of 2.3 keV electrons observed by the OGO-4 satellite. Large field-aligned electron intensities above the 45 keV trapping boundary were observed by Ackerson and Frank (1972) in data from Injun 5. It is reasonable to associate electrons travelling along magnetic field lines with field-aligned currents, such as in the current systems proposed by Boström (1964) and Akasofu and Meng (1969). The first indirect satellite observations of field-aligned currents were reported by Zmuda et al. (1966). Their measurements of transverse magnetic disturbances were explained by Cummings and Dessler (1967) to be the result of currents flowing along magnetic field lines. More recent observations made by Haerendel et al. (1971) on Heos I of perturbations in magnetic field declination further support the results of Armstrong and Zmuda (1970) and the model of Boström (1968).

Electrons from 2 to 18 keV with pitch angle distributions peaked near 0^{o} have been observed in sounding rocket data by Cloutier et al. (1970) and Vondrak et al. (1971). On other rocket flights, field-aligned electrons were observed at 1 keV by Chase (1970) and at 5 keV by O'Brien and Reasoner (1971). Enhanced field-aligned fluxes at the poleward edge of auroral forms were reported by Choy et al. (1971), for 3 to 7 keV electrons, and by Whalen and McDiarmid (1972) for 0.55 keV electrons. Enhancements of 0^{o} pitch angle electrons were also observed by Whalen and McDiarmid at energies up to 9 keV through much of their rocket flight.

This paper presents a synoptic study of field-aligned precipitation events observed by the OGO-4 satellite during a full 4π precession of the satellite orbital plane in magnetic local time (MLT). New information on the morphology of field-aligned precipitation, its nature, and relationships between this phenomenon and other geophysical events will be discussed using data collected during a 16 month period.

THE EXPERIMENT

Launch of the OGO-4 satellite occurred on 28 July 1967. The satellite achieved a nearly circular low-altitude polar orbit with a 908 km apogee and a perigee of 412 km. This orbit had an initial inclination of 86°, which, combined with the motion of the earth around the sun, caused a precession of the orbital plane from its initial dusk-dawn orientation through all local times at the rate of about $1\frac{1}{2}^{\circ}$ per day. Thus the satellite passed through all local times every 120 days, so that by 20 November 1968 a complete 4π precession in local time had been achieved.

The OGO-4 Auroral Particles Experiment (Hoffman and Evans, 1967) consisted of an array of 8 detectors, each comprised of an electrostatic analyzer for species and energy selection and a Bendix channel electron multiplier as the particle detector (Evans, 1965). Four of the detectors, (the "energy detectors"), were positioned to point radially away from the earth and measured either electrons or protons in narrow energy bands centered at 0.7, 2.3, 7.3, and 23.8 keV. Three other detectors (the "angle detectors",) which measured charged particles only at 2.3 keV were positioned 30°, 60°, and 90° from the earth-spacecraft vector; the

eighth detector served as a background detector. Each of the "energy" and "angle" detectors had bandpasses of - 13% and + 19% about their center energy. In the northern high-latitude regions where all of the data used for this study were taken, the energy detectors were oriented approximately parallel to the local magnetic field, and thus measured particles with pitch angles near 0^{o}, while the 2.3 keV, 60^{o} detector measured particles with pitch angles near 60^{o}.

EXAMPLE DATA

We first show an example of precipitating electrons measured near local dawn during a period of moderate magnetic disturbance. One-second averaged fluxes of 0.7 and 2.3 keV electrons are plotted (with background subtracted) in Figure 1, as well as the ratio of the flux of 2.3 keV electrons at 0^{o} pitch angle to that at 60^{o}. The pronounced structure evident in the fluxes of 0.7 keV electrons during this pass has previously been discussed (Hoffman and Berko, 1971) and has been termed 'burst' precipitation (Hoffman and Evans, 1968). The term burst was chosen as being descriptive of the appearance of the data and not necessarily to imply temporal behavior.

Two properties typical of the field-aligned electrons observed by OGO-4 are very prominent in Pass 6558. First, the several periods when the 2.3 keV flux at 0^{o} greatly exceeded the 2.3 keV flux at 60^{o} were of generally short time duration, seldom lasting for more than one or two seconds (the "width" of each bar in the histogram is very close to one second). Second, these periods of field-aligned precipitation coincided

with peaks in the fluxes of both 2.3 and 0.7 keV electrons. Maximum anisotropy occurred at 1829:45 UT at 77.9°, when the ratio of 0° to 60° flux reached 14.8, and the differential flux of 2.3 keV electrons at 0° reached a peak for this pass of $\sim 3 \times 10^9$. This maximum field-aligned peak was observed to last for 5 seconds. From 1830:48 to 1830:55, the ratio remained greater than one; however, only three of the one-second periods of data in this interval had 0° to 60° 2.3 keV flux ratios greater than or equal to two.

A portion of a near-dusk pass which had several periods of field-aligned precipitation is shown in Figure 2. This pass had only three periods of highly anisotropic fluxes, the first two of which, at 0921:36 and 0921:52, were observed to last for only one second. The field-aligned burst at 0921:36 occurred simultaneously with a peak of $\sim 3 \times 10^8$ in the flux of 2.3 keV electrons at 0°, while the second, at 0921:52, occurred together with a smaller peak flux of $\sim 6 \times 10^7$. From 0922:01 to 0922:07, the measured 2.3 keV precipitation was very much field-aligned, and the 2.3 keV fluxes at 0° were primarily greater than 10^8. During this time period, the peak flux of 0.7 keV electrons was also detected.

An interesting example of data collected during a strong magnetospheric disturbance is the portion of Pass 4351 shown in Figure 3. In the high latitude portion of this near-midnight pass the fluxes at 0.7 keV and 2.3 keV were fairly low, structureless, and very isotropic. The fluxes began increasing and fluctuating at 1604:16, but the first appreciably anisotropic period did not begin until 1604:36, coinciding with a moderate peak in the 2.3 keV flux. Small, short duration anisotropies

appeared from 1604:54 to 1606:37, where a large peak in the 2.3 keV flux began in coincidence with the beginning of a seven second period of anisotropy, with the ratio of 0^o to 60^o 2.3 keV flux attaining a peak value just greater than 5 during this time interval. Although the figure ends at 1607:13, this data transmission continued with substantially the same levels of isotropic fluxes until 1607:56, at which time the satellite was just south of $\Lambda = 61^o$.

SPATIAL DISTRIBUTIONS

All available electron data from the OGO-4 Auroral Particles Experiment which were taken during the time interval 30 July 1967 through 20 November 1968 were considered in determining the spatial distributions. Where necessary, background was subtracted from the raw counting rates, which were then converted into one-second average particle fluxes, each of which was considered to be a precipitation event. For all cases where the 2.3 keV flux at 0^o exceeded $\sim 2 \times 10^7$, magnetic local time and invariant latitude (Λ) were computed. Each of these "events" with $\Lambda \geq 60^o$ were sorted into spatial "elements", one hour wide in magnetic local time by $2\frac{1}{2}^o$ in Λ, except for $\Lambda \geq 85^o$, where the latitudinal extent was 5^o (see for example Hoffman and Berko, 1971).

For every event in the 16 month data base, the ratio of 0^o - 2.3 keV flux to 60^o - 2.3 keV flux was calculated. An event was considered to be field-aligned only if this ratio was greater than or equal to 2.0 (see Appendix A). Less than 2% of almost 120,000 events were found to meet this criteria. Systematic biases in the distribution of data due to OGO-4 operational procedures were eliminated by mornalization to account for

uneven coverage in magnetic local time. This yielded a distribution of all precipitation events with most of the precipitation occurring from 19 hours, through midnight, to about 10 hours MLT, in a pattern similar to that presented by Hoffman (1969) for electron precipitation in the several keV energy range.

The normalized distribution of the field-aligned precipitation events under all magnetic conditions is given in Figure 4 in a magnetic local time-invariant latitude polar coordinate projection. This distribution is oval in shape, with the highest number of field-aligned (FA) events in the element extending from 23 to 24 hours MLT and from $\Lambda = 70^{o}$ to $\Lambda = 72.5^{o}$. Significantly high numbers of FA events occurred in a region extending from 22 hours to 01 hours MLT and 67.5^{o} to 72.5^{o} in Λ. Somewhat lower numbers of FA events were detected in a 5^{o} to 15^{o} wide region roughly symmetric about the meridian plane passing through 23 and 11 hours MLT. The distribution is wider in latitude near midnight than at either its morning or afternoon terminus, and generally includes more high latitude elements in the morning and afternoon quadrants than near midnight.

The very high latitude sector centered at midnight actually had only 6 and 7 FA events in each element, but when normalized, the values became greater than 10. This is not to say that this pie-shaped segment is without meaning, since all the other elements with $\Lambda \geq 85^{o}$ also had about the same high weighting factors. A similar statement is also true for the element from 13 to 14 hours MLT and 82.5^{o} to 85^{o} in Λ. Many

elements below $\Lambda = 65^{o}$, and below $\Lambda = 75^{o}$ from 08 hours to 14 hours MLT, had no field-aligned events at all. The lack of 2.3 keV field-aligned precipitation around local noon is not unexpected, since one generally does not observe significant fluxes of greater than 1 keV electrons at these local times (Burch, 1968; Hoffman, 1969; Heikkila and Winningham, 1971).

In Figure 5, the predominance of FA events around local midnight is easily seen, as well as the generally low number of events around local noon. This figure also shows a higher number of FA events in the pre-midnight quadrant (18 to 24 hours MLT) than in the post-midnight quadrant (24 to 06 hours MLT). Of the total of all FA events, 43.3% occurred in the dusk-to-midnight quadrant and 32.3% in the midnight-to-dawn quadrant. Slightly more events were observed in the noon-to-dusk quadrant than in the dawn-to-noon. The nightside hemisphere as a whole contained 75.6% of all FA events, more than three times as many field-aligned events as were observed in the 12 hours from dawn, through noon, to dusk.

Just as field-aligned events occurred primarily at certain magnetic local times, they were observed more frequently at certain invariant latitudes than at others. Figure 6 shows that more FA events occurred (at all MLT's) in the interval $70^{o} \leq \Lambda < 72.5^{o}$ than in any other interval. At $\Lambda < 67.5^{o}$ and $\Lambda > 77.5^{o}$, the numbers of FA events in each of the $2\frac{1}{2}^{o}$ wide invariant latitude intervals drop to less than 1/3 of the number

in the maximum interval. The maximum number of FA events, 42.2% of the total, occurred in the interval $70^{o} \leq \Lambda < 75^{o}$. Less than 4% of the total number were observed (at all MLTs) at $\Lambda < 65^{o}$, and only 6.1% were detected at $\Lambda \geq 80^{o}$. Thus, considering all MLTs, 2.3 keV field-aligned precipitation is observed primarily at invariant latitudes between 67.5^{o} and 75^{o}.

PARTICLE ENERGIES AND FLUXES

In Figures 1-3, we see that not only are the periods of field-aligned 2.3 keV precipitation associated with generally high 0^{o}-2.3 keV fluxes, but usually also with high 0^{o}-0.7 keV fluxes. Three-point energy spectrums of near 0^{o} pitch angle electrons (for electron energies from 0.7 to 7.3 keV) have been constructed for several of the field-aligned and non-field-aligned periods during Pass 4351 (Figure 3) and are presented in Figure 7. The fluxes of 23.8 keV electrons were consistently too low and obscured by fluctuating background levels to be useful in this study.

Two of the spectrums shown were at times of approximate isotropy, as indicated by the ratio of 0^{o} to 60^{o} 2.3 keV flux (R) having a value near 1. At the time of peak anisotropy in this pass (1604:38), when R=7.93, the flux of 2.3 keV electrons was more than an order of magnitude higher than during the non-field-aligned period at 1604:27. During the lower latitude portion of this midnight pass, both the isotropic and field-aligned spectrums (spectrums 4 and 1 in Figure 7) were considerably harder than the higher latitude spectrums. Spectrum 1 shows a 2.3 keV flux more than 20 times greater than that of spectrum 4, which is quite typical for isotropic periods during this lower latitude portion of Pass 4351.

Averaging over all of the field-aligned and non-field-aligned precipitation events used in this study, average energy spectrums were computed and are presented in Figure 8. Clearly, the field-aligned precipitation is characterized by a harder and more intense energy spectrum. If we assume that no fine structure exists in these two energy spectrums, then we can calculate the average energy of the precipitating electrons between 0.7 and 7.3 keV. The average energy during non-field-aligned precipitation is found to be 1.83 keV, and the average energy during periods of field-aligned precipitation is 1.99 keV.

Field-aligned 2.3 keV electron precipitation is found to be strongly dependent on particle flux, as is evident from the three data examples presented. In Figure 9, we see that the probability of 2.3 keV precipitation being field-aligned increases quite steadily with rising flux of 0^{o} - 2.3 keV electrons. The probability of precipitation being field-aligned increases very rapidly at 0^{o} - 2.3 keV fluxes above $\sim 10^{9}$. There is also a small but noticeable increase in probability of 2.3 keV electrons being field-aligned as the flux of 0^{o} - 0.7 keV electrons rises, becoming significant at fluxes greater than 2×10^{9}.

COMPARISON WITH OPTICAL MEASUREMENTS

Since the field-aligned precipitation occurs primarily in the nightside hemisphere and at times of high particle flux, we looked for an association of field-aligned precipitation with optical aurora in the nighttime hours. To make a meaningful comparison, an optical study was sought which utilized procedures most analogous to those used in determining

the distribution of field-aligned precipitation, i.e., it must be synoptic in nature, occur during a similar epoch of the solar cycle, and have resolution in local time and invariant latitude comparable to the element size of the distribution of field-aligned precipitation.

Optical auroral frequency studies of Feldstein (1966), Lassen (1969), Sandford (1964, 1968), and Stringer and Belon (1967) were each considered. Of these four ground-based studies, the work of Stringer and Belon was the one which best conformed to the established criteria and is thus the most suitable for comparison with our satellite auroral particle observations.

Making use of data acquired by an all-sky camera network based in Alaska during the winter of 1964-65, Stringer and Belon (1967) produced contour maps showing the probabilities of observing discrete, homogeneous, and all auroral forms in 15 minute intervals. It is their isoauroral diagram for all auroral forms which we wish to compare with the distribution of field-aligned precipitation, since data obtained under all magnetic conditions were used in determining the regions of this type of precipitation.

In Figure 10 we shaded the regions from 16 hours, through midnight, to 8 hours local time where the probability of observing all auroral forms presented by Stringer and Belon (1967) was greater than 25%. The heavy lines in these same hours enclose the areas (from Figure 4) where more than at least 30 field-aligned precipitation events were observed. There is clearly a great deal of congruity of these two regions,

especially during the 18 hour to 01 hour local time segment. However, at all local times, except near dawn, most of the field-aligned precipitation occurred poleward of the auroral optical emissions.

This spatial relationship is consistent with sounding rocket observations by Whalen and McDiarmid (1972), who observed auroral electron precipitation to be especially field-aligned as their rocket payload crossed the poleward edge of the visual aurora. Airplane studies of polar cap (i.e., very high latitude) aurora by Eather and Akasofu (1969) indicated that the field-aligned bursts of electrons reported by Hoffman and Evans (1968), and elaborated on in this study, would tend to excite the patches of northern high latitude auroral forms which they observed. Both of these findings are consistent with the results of the comparison made using Figure 10, and suggest that we might seek a possible pattern of field-aligned precipitation occurring at or near the high latitude boundary of auroral particle precipitation in the nightside hours.

An example of this situation is presented in Figure 11, which shows the differential number fluxes of 0.7, 2.3, and 7.3 keV electrons at 0^{o}, as well as the ratio of 0^{o} to 60^{o} fluxes of 2.3 keV electrons. The plot begins when the experiment was turned on at 1020:08, and continues until the high-latitude boundary of 0.7 keV electron precipitation was reached, at 1023:19 during this midnight pass. This latter boundary occurred at $\Lambda = 74.0^{o}$. Similar boundaries for 2.3 and 7.3 keV electrons occurred at 1023:13, at $\Lambda = 73.6^{o}$. The area under the 0^{o} to 60^{o} ratio histogram has been cross-hatched where the 2.3 keV precipitation was field-aligned.

Several features of this figure should be noted. There are two fairly distinct regions of precipitation evident here, a lower latitude region of fairly diffuse, very isotropic fluxes, and a higher latitude region of structured, often anisotropic precipitation (Hoffman and Berko, 1971). The field-aligned fluxes occurred only during the latter portion of the pass, and the last field-aligned portion occurred at the high latitude boundary of 2.3 keV precipitation. From 1021:33 to 1022:03, the beginning of the first field-aligned period at $\Lambda = 69.8^{o}$, the 7.3 keV flux was less than 10^{5}.

Magnetograms from Barrow, College, and Sitka at the time of the pass are presented in the bottom portion of Figure 11, with a letter M indicating the time when each station was at midnight. These indicate that Pass 2590 occurred during the expansion phase of a substorm, which showed up as a 590γ bay at College and a depression of over 650γ in the H component at Barrow.

A search through the OGO-4 data revealed 37 additional passes which traversed the dusk-to-midnight sector during periods of clearly quiet magnetic conditions, or during substorm expansion, as determined from all available ground magnetograms. Each of these 38 passes also had well-defined high latitude particle cutoffs. The latitudinal distribution of near 0^{o} pitch angle electron precipitation for three different energies is shown in Figure 12 for these passes, which are separated into three categories according to substorm activity and the direction of the interplanetary magnetic field (Burch, 1972; Hoffman, 1972).

When the interplanetary magnetic field was directed north and the geomagnetic field was quiet, the high latitude particle cutoffs were at the highest latitudes, and the precipitation was generally isotropic. Only a few of the passes occurring under these "quiet-north" conditions had any appreciable field-aligned precipitation, and all of it was at high latitudes ($\Lambda > 72^{o}$) and often at or near the high latitude boundary of 2.3 keV precipitation.

Those passes shown in the lower left section of the figure occurred when the interplanetary magnetic field, (as observed by Explorers 33 and 35), was directed south, but ground station magnetograms indicated quiet magnetic conditions. No pitch angle anisotropies were observed during any of these pre-breakup passes, but the high latitude particle cutoffs were several degrees lower than typical values (Hoffman, 1969, Burch, 1968).

Passes occurring during the expansion phase of substorms all had field-aligned 2.3 keV precipitation, indicated by a heavy vertical mark across the 2.3 keV "precipitation line", the width of the mark corresponding to the latitudinal extent of the anisotropies. The field-aligned precipitation during these passes was generally at or near the high latitude boundary of auroral electron precipitation. This is especially evident in those passes which occurred during orbits 968, 2988, and 3247. Thus, field-aligned 2.3 keV electron precipitation, especially during times of magnetospheric substorms, is usually associated with the high latitude, or poleward portion of the auroral electron precipitation.

DISCUSSION AND CONCLUSIONS

A synoptic survey of 16 months of data from the OGO-4 Auroral Particles Experiment indicates that field-aligned 2.3 keV electron precipitation at high latitudes is found to occur in a roughly oval-shaped region, with the highest number of field-aligned events observed at about 70^{o} invariant latitude near local midnight. In the nighttime hours, the region of field-aligned precipitation generally coincides with, and extends poleward of, the optically defined auroral region.

The electron energy spectrums during periods of field-aligned 2.3 keV precipitation are harder and considerably more intense than energy spectrums of typical isotropic precipitation. Field-aligned 2.3 keV electron precipitation is most likely to occur when 0^{o} pitch angle 2.3 keV particle fluxes, and to a lesser extent 0^{o}-0.7 keV fluxes, are high, and during post-breakup phases of magnetospheric substorms.

Using the average field-aligned fluxes shown in Figure 8, the current density in the bandpasses of the detectors is calculated to be $\sim 3.05 \times 10^{-6}$ amp/m^2. A field-aligned current of this magnitude would fit in well with the models of Boström (1968) and Akasofu and Meng (1969), and is of the order of magnitude of currents reported by several authors in the recent literature (Choy et al., 1971; Cloutier et al., 1970; Frank, 1971; Vondrak et al., 1971).

A comparison of the normalized distribution of all field-aligned events can be made with the locations of transverse magnetic disturbances presented by Zmuda et al (1970). Although their data were primarily from the dayside because of the normal ground-station working hours and

the solar-only mode capability of the satellite 1963-38C, their region of transverse magnetic disturbances, observed in the period February 1964 through May 1968, showed the same tendency of lying at higher latitudes in the dayside hours than near midnight as the distribution of field-aligned precipitation shown in Figure 4. At midnight, under quiet magnetic conditions ($Kp \leq 2^+$), their region of transverse disturbances, which they associate with field-aligned currents, lay between 69^o and 72^o Λ, also in excellent agreement with the peak values of Figure 4. To estimate some properties of the currents producing the magnetic perturbations, they used an infinite-sheet current approximation which required a particle flux of $0.12 - 3.5 \times 10^9$ particles/cm^2-sec. Electron fluxes of this magnitude have frequently been observed at 0.7 keV in the dayside hours by OGO-4 (Hoffman and Berko, 1971), and at lower energies by Heikkila and Winningham (1971) and Frank (1971), which implies that the (dayside) field-aligned currents of Zmuda et al. are due to particles with energies less than 2.3 keV.

As seen by OGO-4, field-aligned precipitation appears as a generally short-time-duration phenomenon, seldom appearing continuously for more than 5 to 10 seconds in the satellite data. Whether this is really a temporal effect (Hoffman and Evans, 1968; Chase, 1970; O'Brien and Reasoner, 1971), or a spatial effect (Eather and Akasofu, 1969; Cloutier et al., 1970; Choy et al., 1971; Whalen and McDiarmid, 1972), or some combination of spatial and time varying effects (D. S. Evans, private communication, 1972), cannot easily be determined using data obtained from a satellite moving at $\sim$ 7.5 km/sec. Determination of the mechanism responsible for field-aligned auroral zone precipitation is strongly dependent on whether spatial or temporal processes are dominant.

APPENDIX A

The reasons for considering an event to be field-aligned only if the 0^{o}-2.3 keV flux exceeded $\sim 2 \times 10^{7}$ electrons/cm^{2}-sec-ster-keV and the ratio of 0^{o} to 60^{o} 2.3 keV flux was greater than or equal to 2.0 are as follows. Fluxes less than 2×10^{7} represented as few as 7 counts per second (N). At this counting rate, the statistical error ($\sqrt{N}/N$) is 38%, and equal 0^{o} and 60^{o} counting rates of 7 counts per second would then yield a combined uncertainty of $\pm$ 76% in the ratio, giving a 0^{o} to 60^{o} flux ratio of 1.0 ± 0.76. Therefore, choosing ratios greater than or equal to 2.0 insures that only statistically significant field-aligned events were included in the distribution for all fluxes greater than $\sim 2 \times 10^{7}$.

ACKNOWLEDGMENTS

I am especially grateful to Dr. Robert A. Hoffman for his continuing guidance and advice and many helpful suggestions throughout the course of this study. Discussions with Drs. J. L. Burch, Y. C. Whang, and A. D. Johnstone have proven beneficial in developing the methods used to perform this study and in interpreting the results. The magnetometer data used in this paper were obtained from the National Space Science Data Center at Goddard Space Flight Center.

REFERENCES

Ackerson, K. L., and L. A. Frank, Correlated satellite measurements of low-energy electron precipitation and ground-based observations of a visible auroral arc, J. Geophys. Res., 77, 1128, 1972.

Akasofu, S.-I., and C.-I. Meng, A study of polar magnetic substorms, J. Geophys. Res., 74, 293, 1969.

Armstrong, J. C., and A. J. Zmuda, Field-aligned current at 1100 km in the auroral region measured by satellite, J. Geophys. Res., 75, 7122, 1970.

Boström, R., A model of the auroral electrojet, J. Geophys. Res., 69, 4983, 1964.

Boström, R., Currents in the ionosphere and magnetosphere, Ann. Geophys., 24, 681, 1968.

Burch, J. L., Low-energy electron fluxes at latitudes above the auroral zone, J. Geophys. Res., 73, 3585, 1968.

Burch, J. L., Precipitation of low-energy electrons at high latitudes: Effects of substorms, interplanetary magnetic field and dipole tilt angle, submitted to J. Geophys. Res., 1972.

Chase, L. M., Energy spectra of auroral zone particles, J. Geophys. Res., 75, 7128, 1970.

Choy, L. W., R. L. Arnoldy, W. Potter, P. Kintner, and L. J. Cahill, Jr., Field-aligned particle currents near an auroral arc, J. Geophys. Res., 76, 8279, 1971.

Cloutier, P. A., H. R. Anderson, R. J. Parks, R. R. Vondrak, R. J. Spiger, and B. R. Sandel, Detection of geomagnetically aligned currents associated with an auroral arc., J. Geophys. Res., 75, 2595, 1970.

Cummings, W. D., and A. J. Dessler, Field-aligned currents in the magnetosphere, J. Geophys. Res., 72, 1007, 1967.

Eather, R. H., and S.-I. Akasofu, Characteristics of polar cap auroras, J. Geophys. Res., 74, 4794, 1969.

Evans, D. S., Low energy charged particle detection using the continuous channel electron multiplier, Rev. Sci. Instr., 36, 375, 1965.

Feldstein, Y. I., Peculiarities in the auroral distribution and magnetic disturbance distribution in high latitudes caused by the asymmetrical form of the magnetosphere, Planet. Space Sci., 14, 121, 1966.

Frank, L. A., Plasma in the earth's polar magnetosphere, J. Geophys. Res., 76, 5202, 1971.

Haerendel, G., P. C. Hedgecock, and S.-I. Akasofu, Evidence for magnetic field aligned currents during the substorms of March 18, 1969, J. Geophys. Res., 76, 2382, 1971.

Heikkila, W. J., and J. D. Winningham, Penetration of magnetosheath plasma to low altitudes through the dayside magnetospheric cusps, J. Geophys. Res., 76, 883, 1971.

Hoffman, R. A., Low energy electron precipitation at high latitudes, J. Geophys. Res., 74, 2425, 1969.

Hoffman, R. A., Electron precipitation patterns and substorm morphology, EOS, Trans. AGU, 53, 360, 1972.

Hoffman, R. A., and D. S. Evans, OGO-4 auroral particles experiment and calibrations, Goddard Space Flight Center Preprint, X-611-67-632, 1967.

Hoffman, R. A., and D. S. Evans, Field aligned electron bursts at high latitudes observed by OGO-4, J. Geophys. Res., 73, 6201, 1968.

Hoffman, R. A., and F. W. Berko, Primary electron influx to dayside auroral oval, J. Geophys. Res., 76, 2967, 1971.

Lassen, K., Polar cap emissions, Atmospheric Emissions, ed. B. M. McCormac and A. Omhold, Van Nostrand Reinhold Co., New York, p. 63, 1969.

O'Brien, B. J., and D. L. Reasoner, Measurements of highly collimated short-duration bursts of auroral electrons and comparison with existing auroral models, J. Geophys. Res., 76, 8258, 1971.

Sandford, B. P., Aurora and airglow intensity variations with time and magnetic activity at southern high latitudes, J. Atmosph. Terr. Phys., 26, 749, 1964.

Sandford, B. P., Variations of auroral emissions with time, magnetic activity, and the solar cycle, J. Atmosph. Terr. Phys., 30, 1921, 1968.

Stringer, W. J., and A. E. Belon, The morphology of the IQSY auroral oval: 1. Interpretation of isoauroral diagrams., J. Geophys. Res., 72, 4415, 1967.

Vondrak, R. R., H. R. Anderson, and R. J. Spiger, Rocket-based measurement of particle fluxes and currents in an auroral arc, J. Geophys. Res., 76, 7701, 1971.

Whalen, B. A., and I. B. McDiarmid, Observations of magnetic-field-aligned auroral electron precipitation, J. Geophys. Res., 77, 191, 1972.

Zmuda, A. J., J. H. Martin, and F. T. Heuring, Transverse magnetic disturbances at 1100 kilometers in the auroral region, J. Geophys. Res., 71, 5033, 1966.

Zmuda, A. J., J. C. Armstrong, and F. T. Heuring, Characteristics of transverse magnetic disturbances observed at 1100 kilometers in the auroral oval, J. Geophys. Res., 75, 4757, 1970.

FIGURE CAPTIONS

Figure 1. One-second average fluxes of 0.7 and 2.3 keV, near 0^{o} pitch angle electrons, and the ratio of 0^{o} - 2.3 keV to 60^{o} - 2.3 keV electron fluxes, for a near dawn pass during a moderately disturbed period. Universal time and orbital data are given at the bottom of the figure.

Figure 2. Same as Figure 1, for a pass near dusk.

Figure 3. Same as Figure 1, for a midnight pass during a period of high magnetic activity.

Figure 4. Normalized distribution of field-aligned 2.3 keV electron precipitation events. See text for criteria used to define field-aligned events, including data, and performing normalization.

Figure 5. Distribution of field-aligned events in magnetic local time, at all invariant latitudes.

Figure 6. Percent of field-aligned events, at all local times, as a function of invariant latitude, from 60^{o} to 90^{o}.

Figure 7. Energy spectrums for four periods during Pass 4351 (Figure 3). Spectrums 1 and 2 were obtained during field-aligned precipitation events. Spectrums 3 and 4 were obtained during times of isotropic fluxes.

Figure 8. Average three point energy spectrums for all field-aligned and all non-field-aligned precipitation events used in this study.

Figure 9. Probability of 2.3 keV precipitation being field-aligned as a function of 0^{o} particle flux at 0.7 and 2.3 keV.

Figure 10. Polar projection of the regions of high numbers of field-aligned events in the nighttime hours in comparison with the region of high probability of all auroral forms (Stringer and Belon, 1967) during the same hours.

Figure 11. One-second average fluxes of 0.7, 2.3, and 7.3 keV near 0^{o} pitch angle electrons, and the ratio of 0^{o}-2.3 keV to 60^{o}-2.3 keV electron fluxes, for a midnight pass during substorm expansion. Periods of field-aligned precipitation are indicated by cross-hatching. Three magnetograms for the time period are shown with a heavy vertical line indicating the time when Pass 2590 occurred.

Figure 12. Latitudinal distribution of auroral electron precipitation at 3 energies for 38 passes in the dusk-to- midnight sector which had well-defined high-latitude particle cutoffs. Field-aligned precipitation is indicated by dark vertical bars. See text for details.

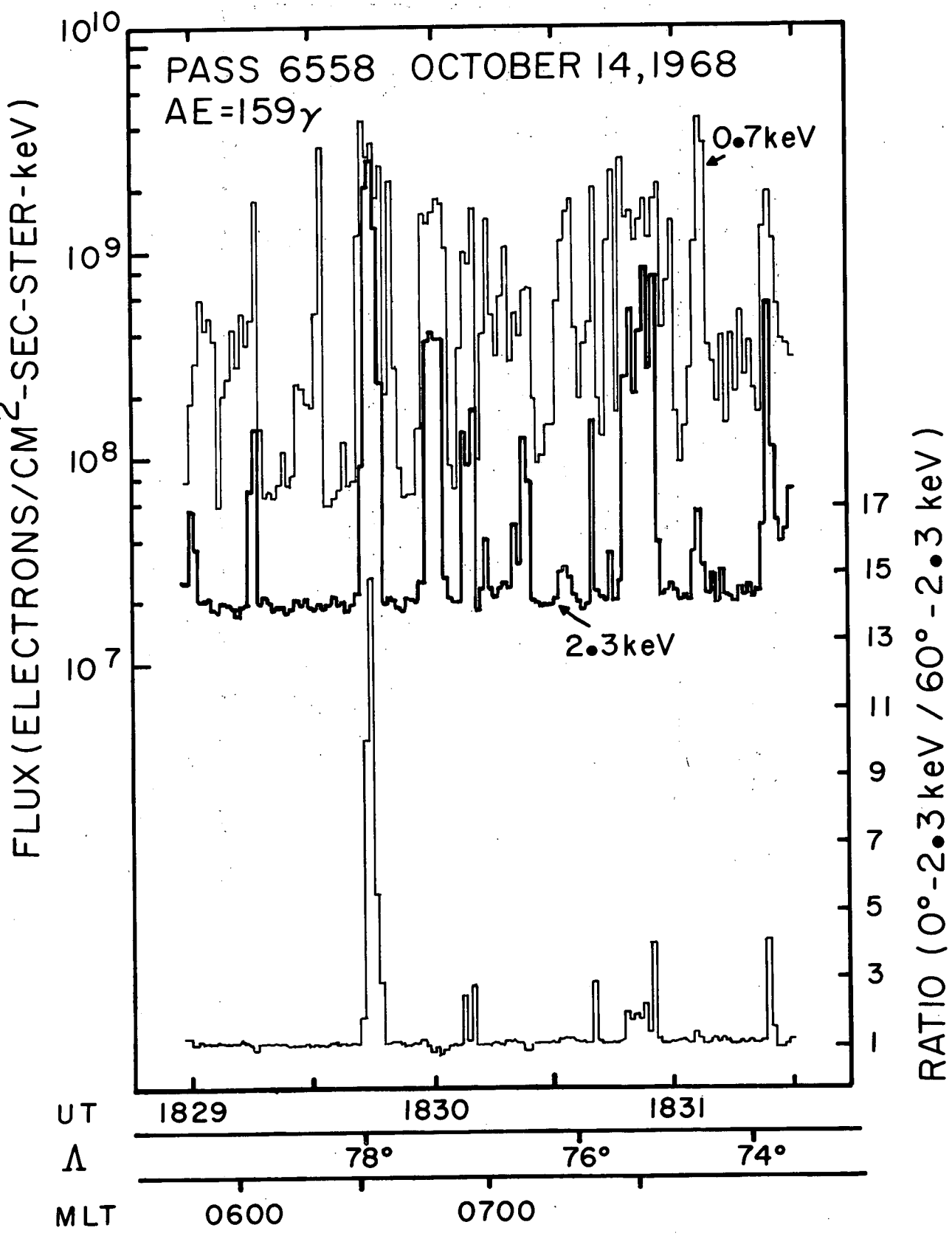
PASS 6558 OCTOBER 14, 1968
AE=159γ
0.7keV
2.3keV
FLUX (ELECTRONS/CM²-SEC-STER-keV)
RATIO (0°-2.3keV / 60°-2.3 keV)
10¹⁰
10⁹
10⁸
10⁷
17
15
13
11
9
7
5
3
1
UT
1829
1830
1831
Λ
78°
76°
74°
MLT
0600
0700

Figure 1

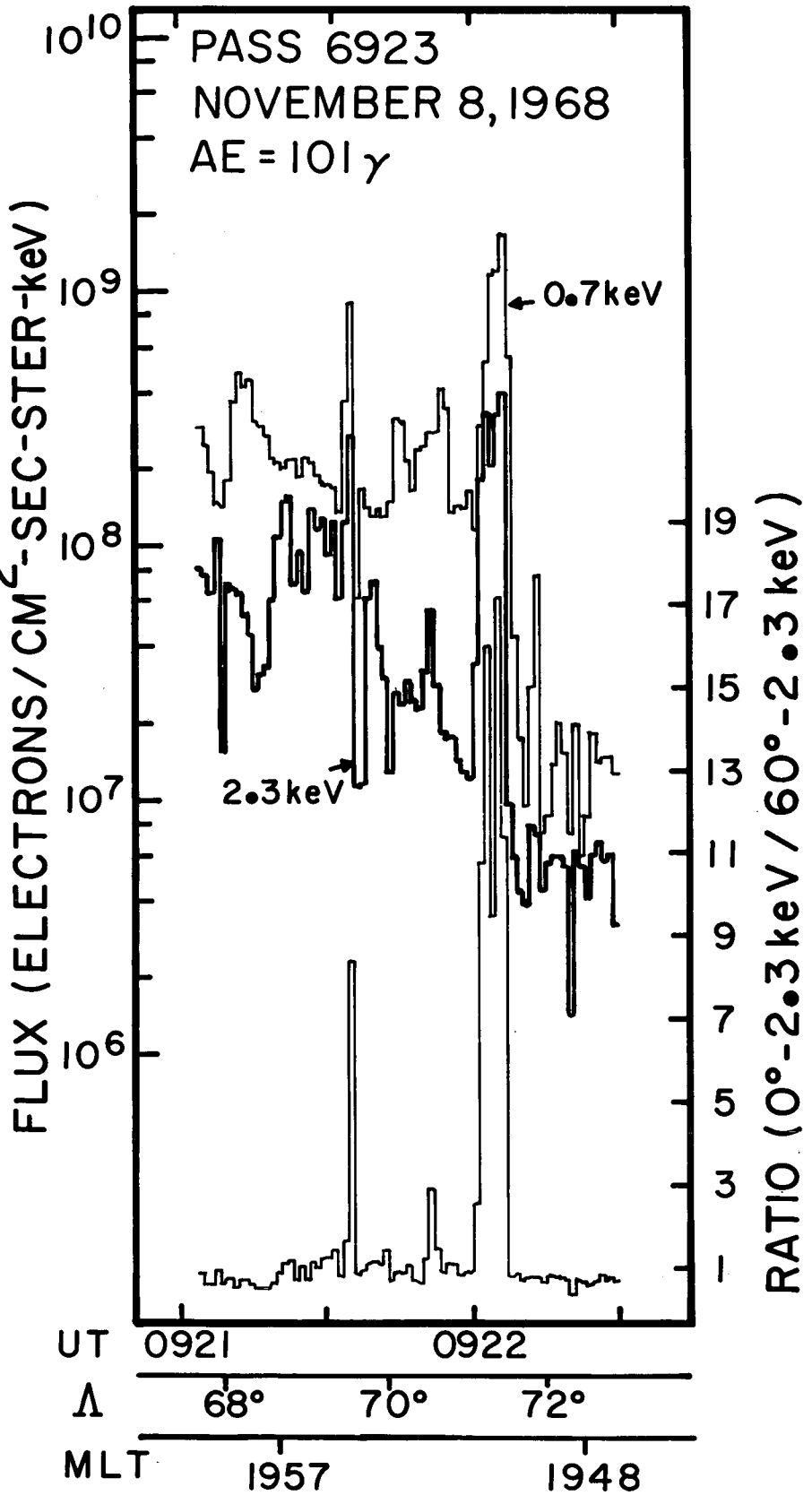
PASS 6923
NOVEMBER 8, 1968
AE = 101 γ
0.7keV
2.3keV
FLUX (ELECTRONS/CM²-SEC-STER-keV)
RATIO (0°-2.3keV / 60°-2.3keV)
UT
0921
0922
Λ
68°
70°
72°
MLT
1957
1948

Figure 2

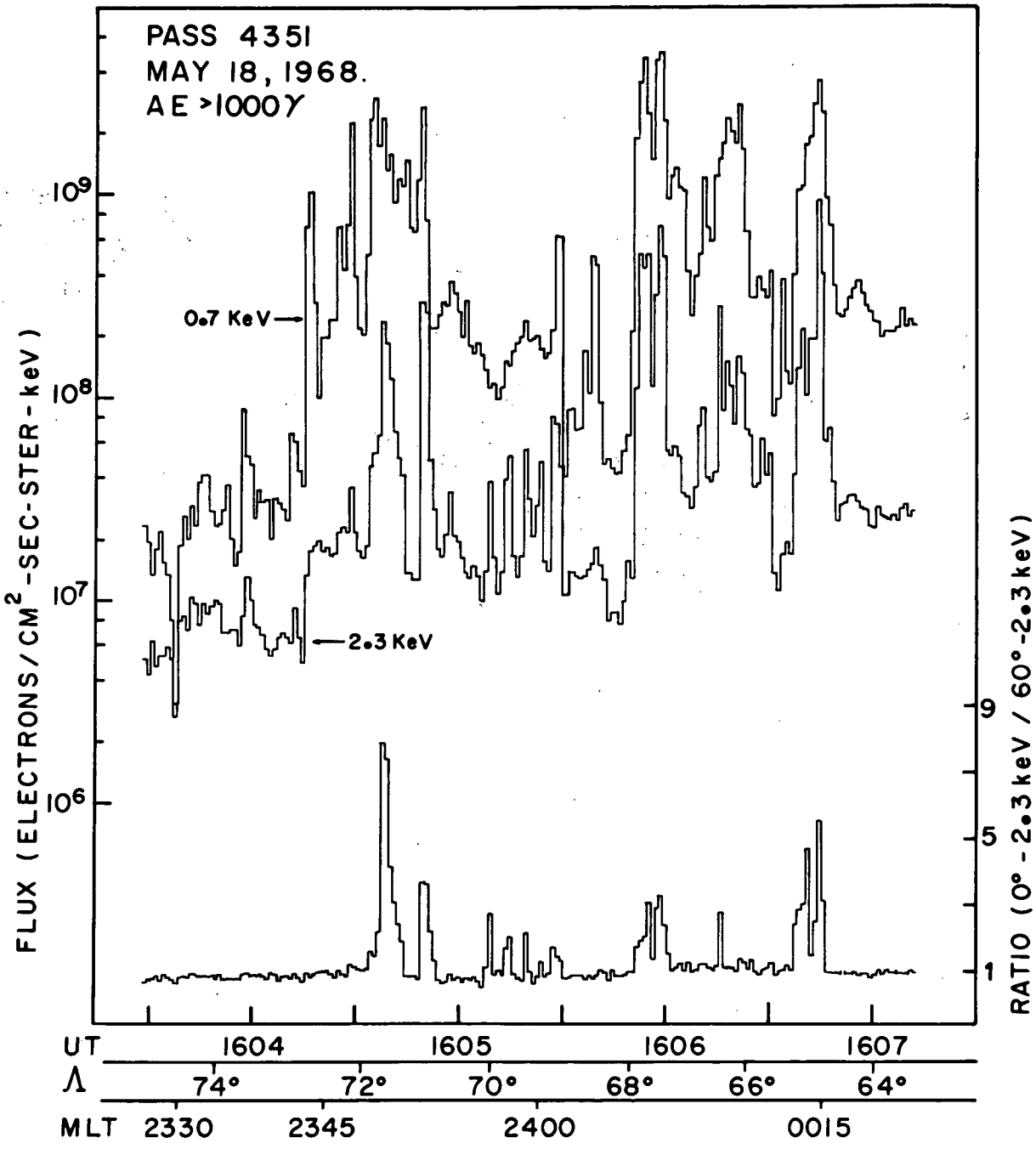
PASS 4351
MAY 18, 1968.
AE >1000γ
0.7 KeV
2.3 KeV
FLUX (ELECTRONS/CM²-SEC-STER-keV)
RATIO (0°-2.3 keV / 60°-2.3 keV)
UT
1604
1605
1606
1607
Λ
74°
72°
70°
68°
66°
64°
MLT
2330
2345
2400
0015

Figure 3

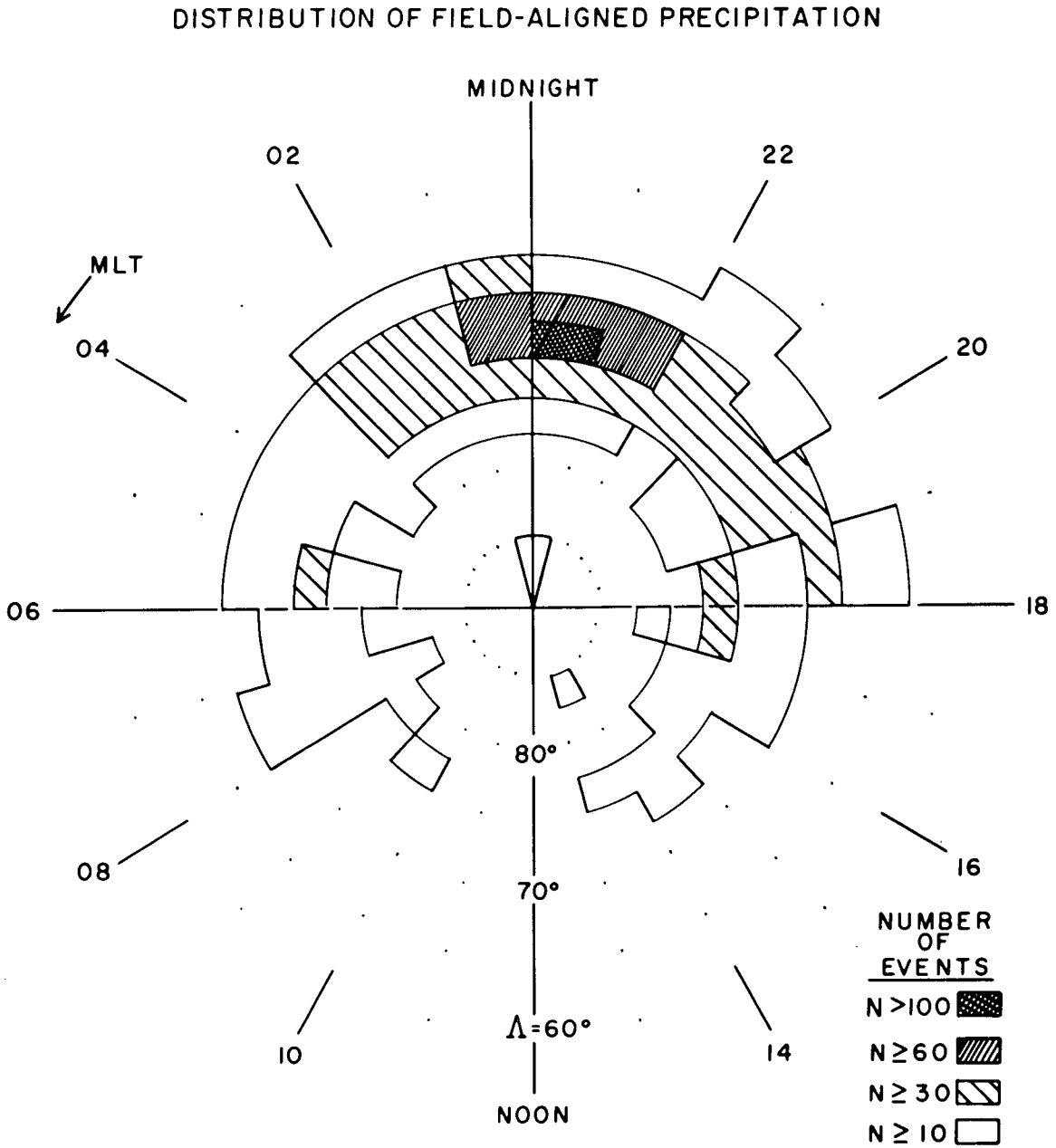
DISTRIBUTION OF FIELD-ALIGNED PRECIPITATION
MIDNIGHT
02
22
MLT
04
20
06
18
80°
08
16
70°
NUMBER OF EVENTS
N >100
N ≥60
N ≥30
N ≥10
Λ=60°
10
14
NOON

Figure 4

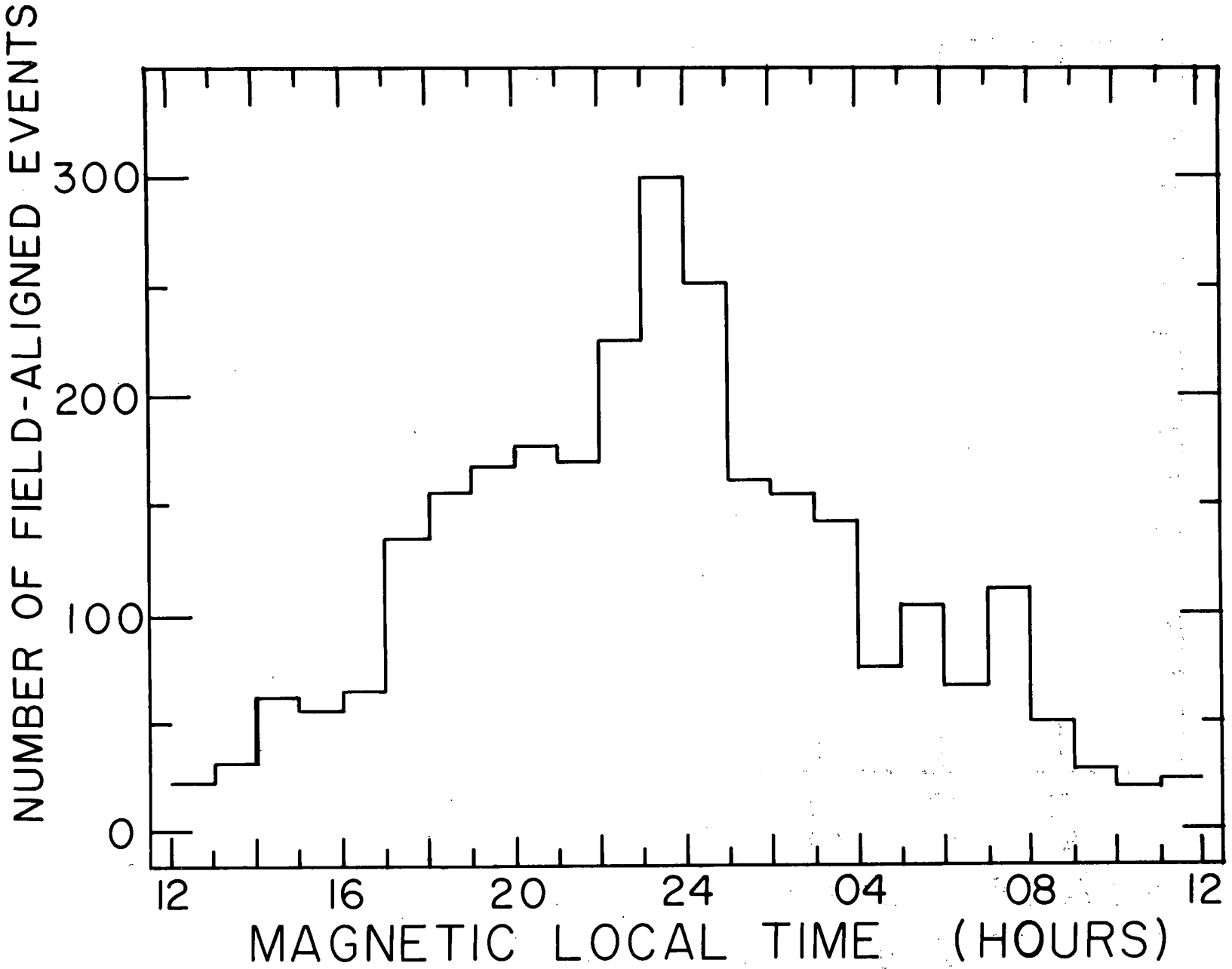
NUMBER OF FIELD-ALIGNED EVENTS
300
200
100
0
12
16
20
24
04
08
12
MAGNETIC LOCAL TIME (HOURS)

Figure 5

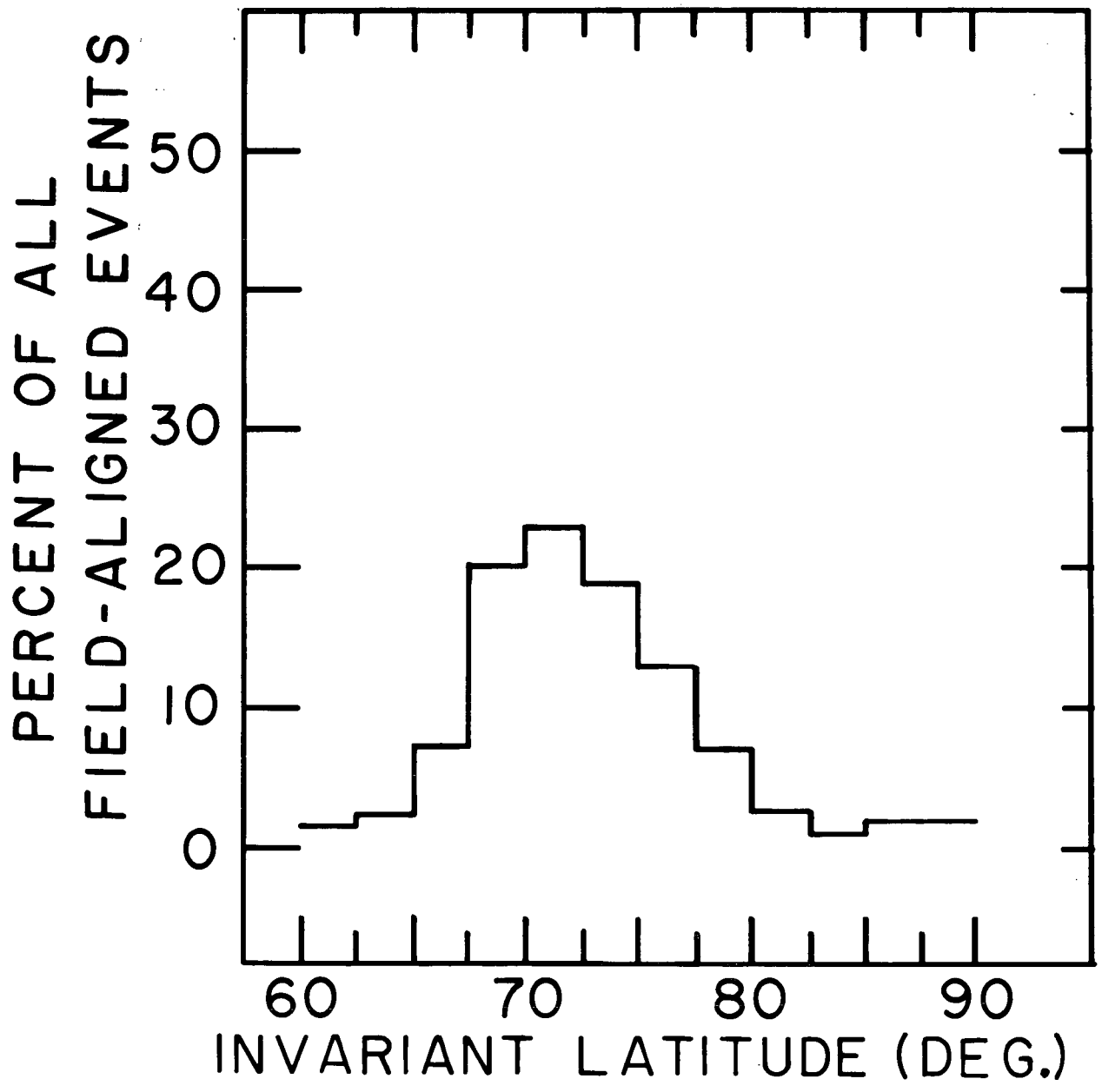
PERCENT OF ALL
FIELD-ALIGNED EVENTS
0
10
20
30
40
50
60
70
80
90
INVARIANT LATITUDE (DEG.)

Figure 6

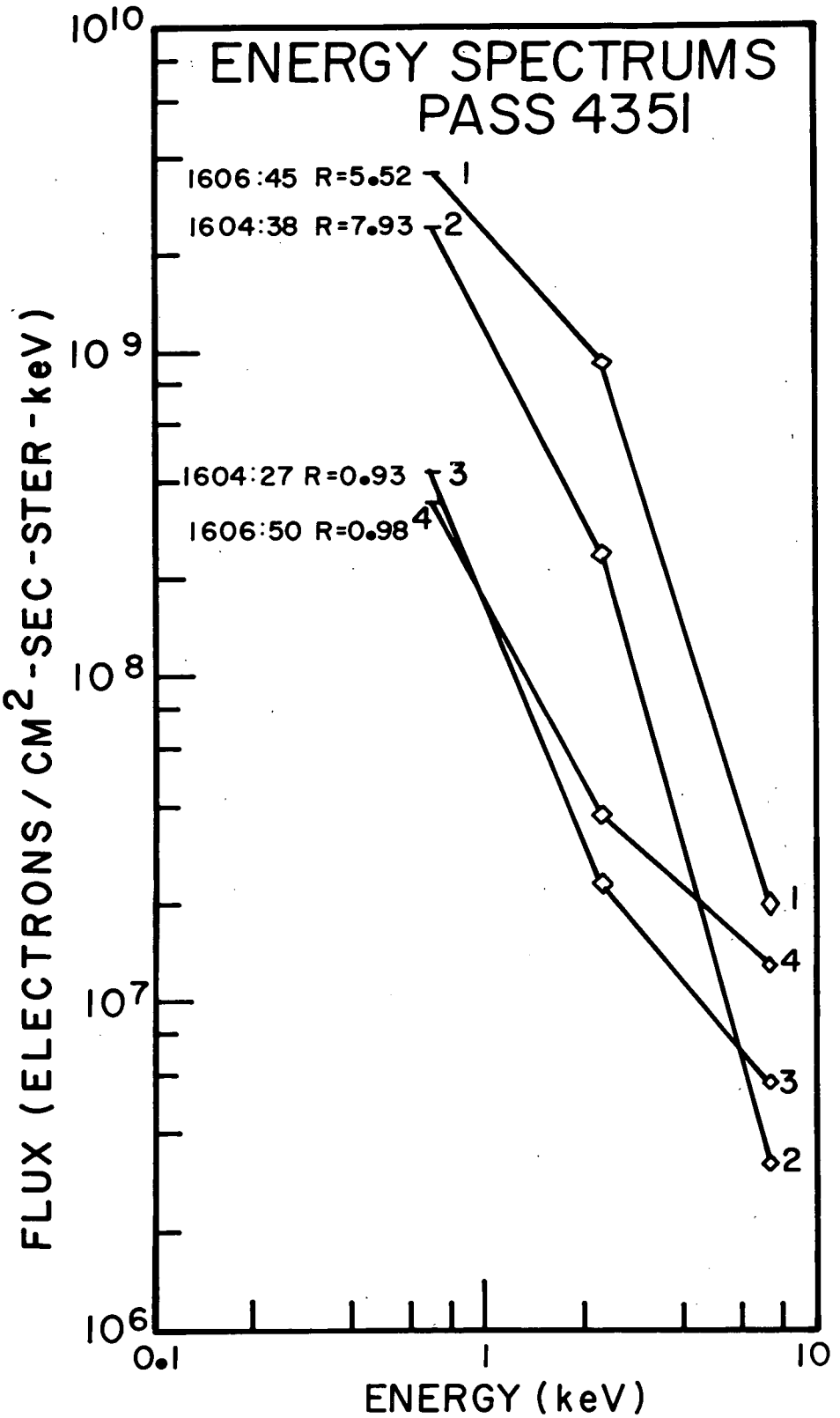
ENERGY SPECTRUMS
PASS 4351
1606:45 R=5.52
1604:38 R=7.93
1604:27 R=0.93
1606:50 R=0.98
1
2
3
4
10^{10}
10^{9}
10^{8}
10^{7}
10^{6}
FLUX (ELECTRONS / CM^2-SEC-STER-keV)
0.1
1
10
ENERGY (keV)

Figure 7

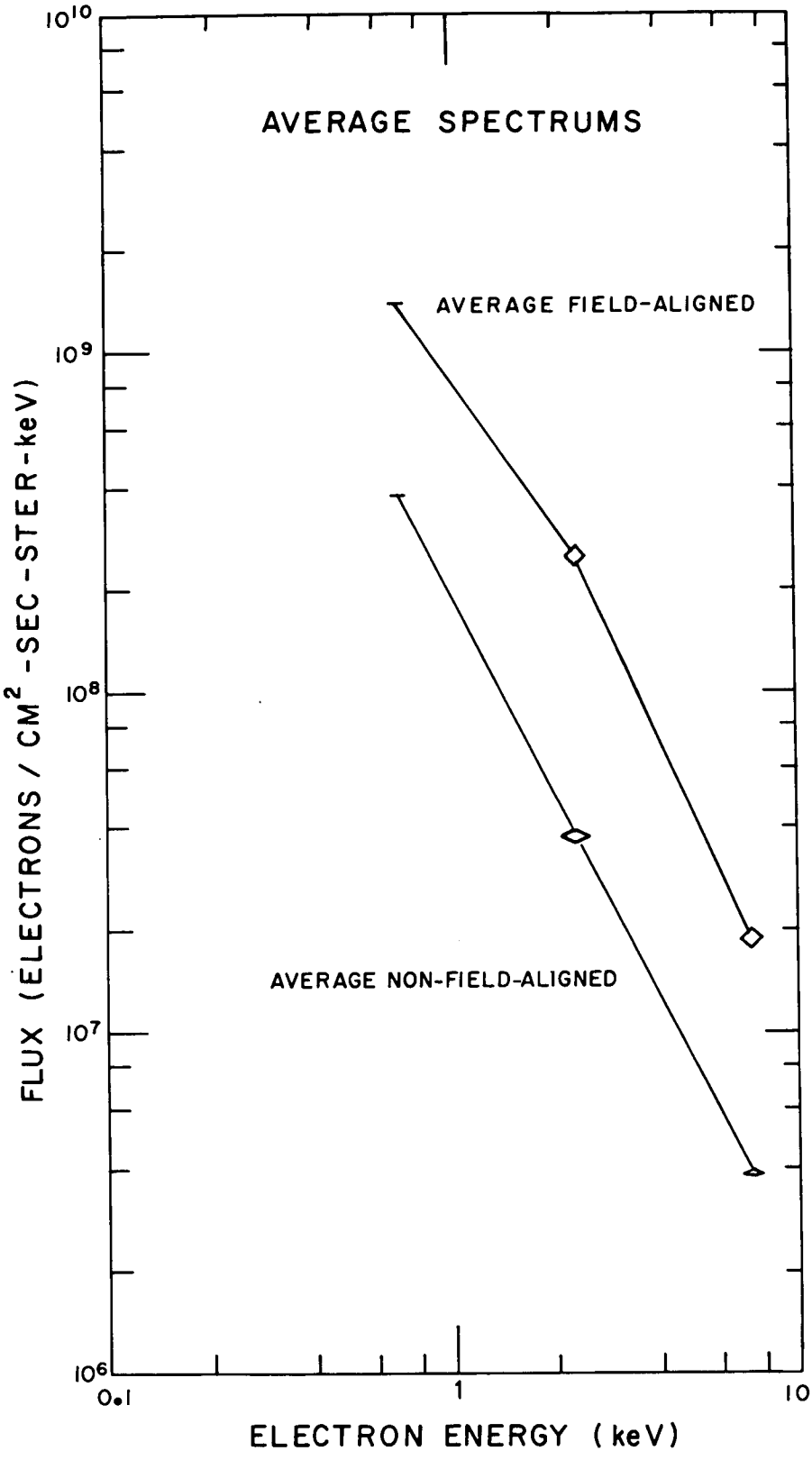
AVERAGE SPECTRUMS
AVERAGE FIELD-ALIGNED
AVERAGE NON-FIELD-ALIGNED
FLUX (ELECTRONS / CM^2-SEC-STER-keV)
ELECTRON ENERGY (keV)
10^{10}
10^9
10^8
10^7
10^6
0.1
1
10

Figure 8

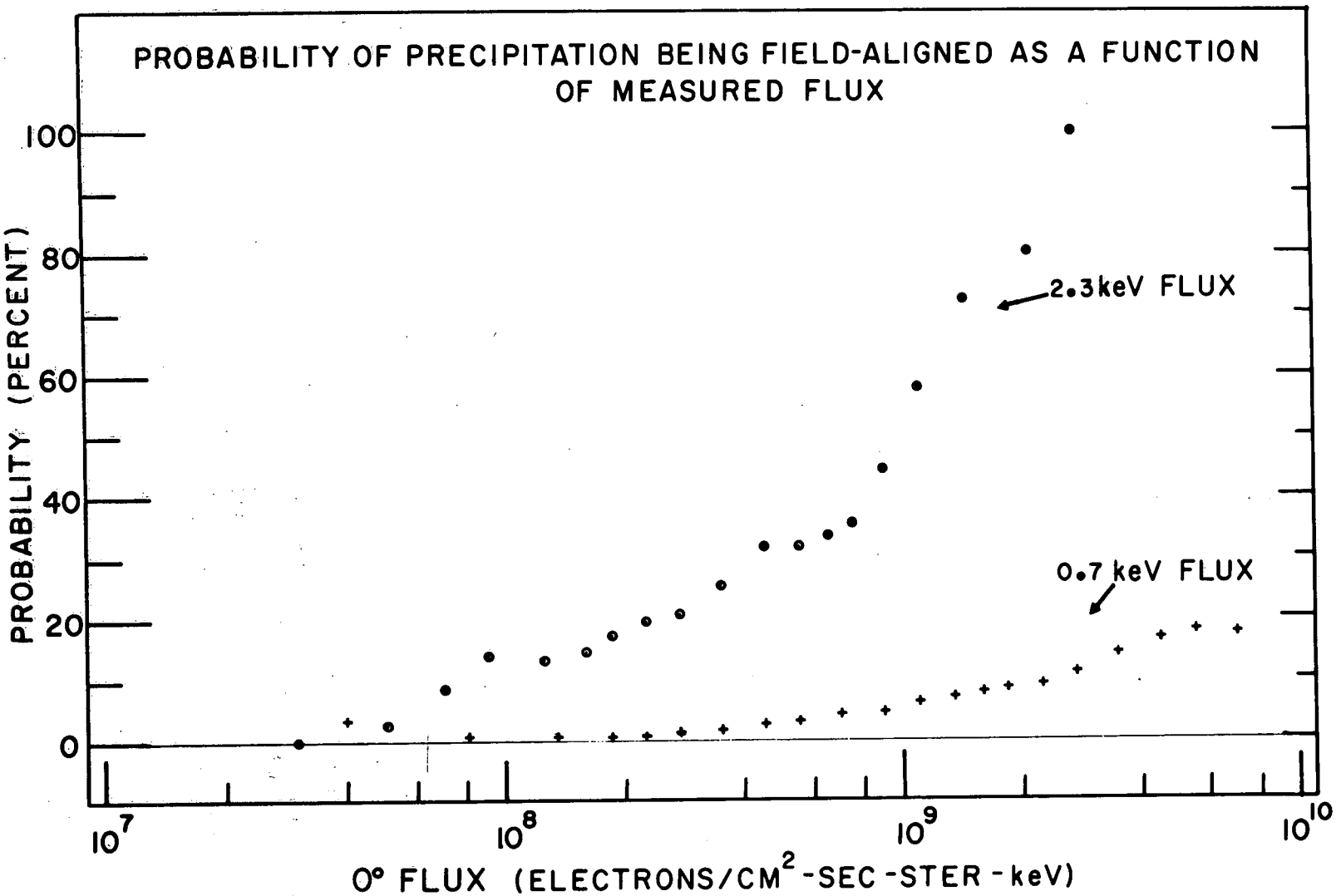
PROBABILITY OF PRECIPITATION BEING FIELD-ALIGNED AS A FUNCTION OF MEASURED FLUX
PROBABILITY (PERCENT)
100
80
60
40
20
0
2.3keV FLUX
0.7 keV FLUX
10^7
10^8
10^9
10^{10}
0° FLUX (ELECTRONS/CM^2-SEC-STER-keV)

Figure 9

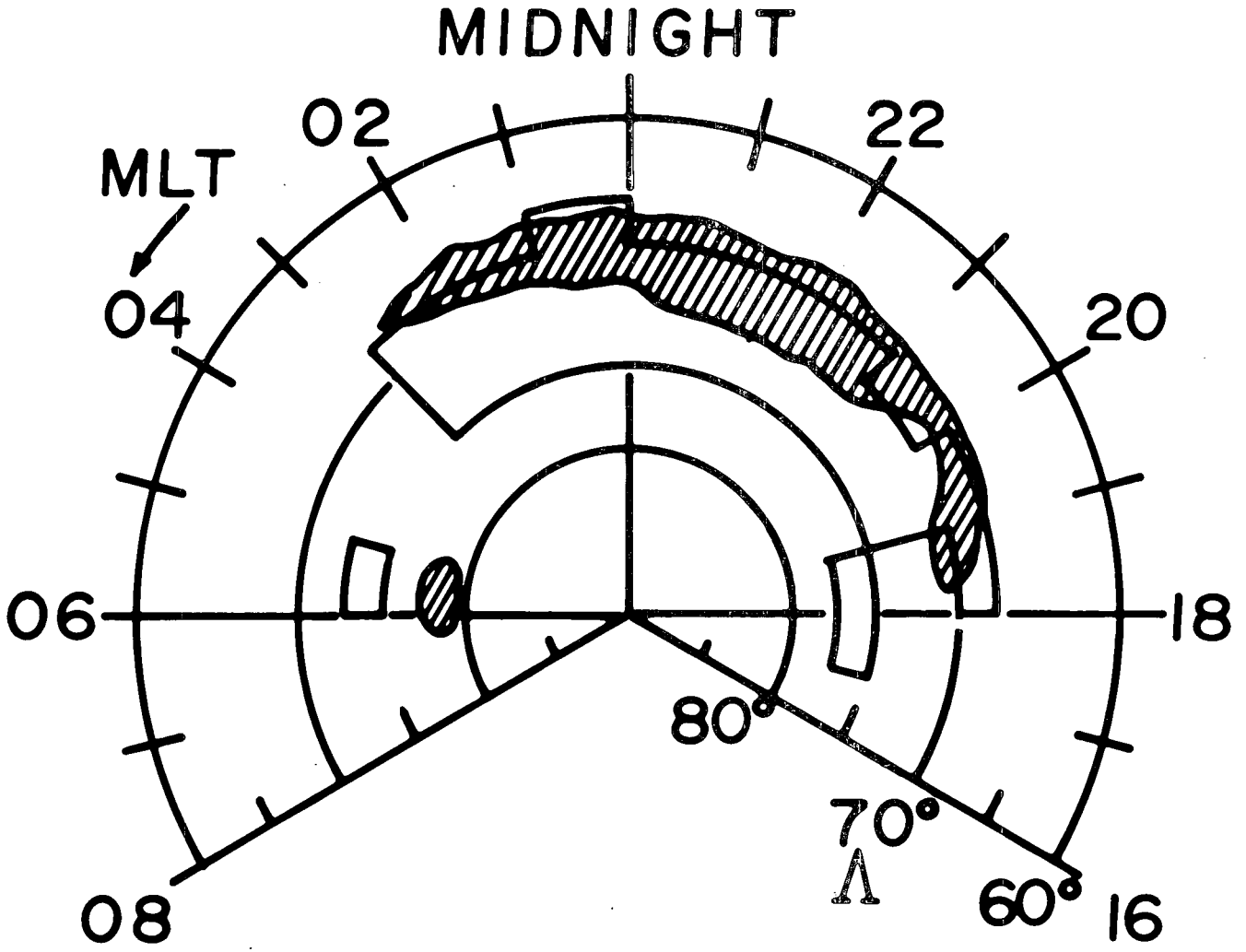
MIDNIGHT
MLT
02
22
04
20
06
18
80°
70°
Λ
60°
08
16
N ≥ 30 FIELD-ALIGNED EVENTS
ALL AURORAL FORMS PROBABILITY ≥ 25%
(STRINGER AND BELON, 1967)

Figure 10

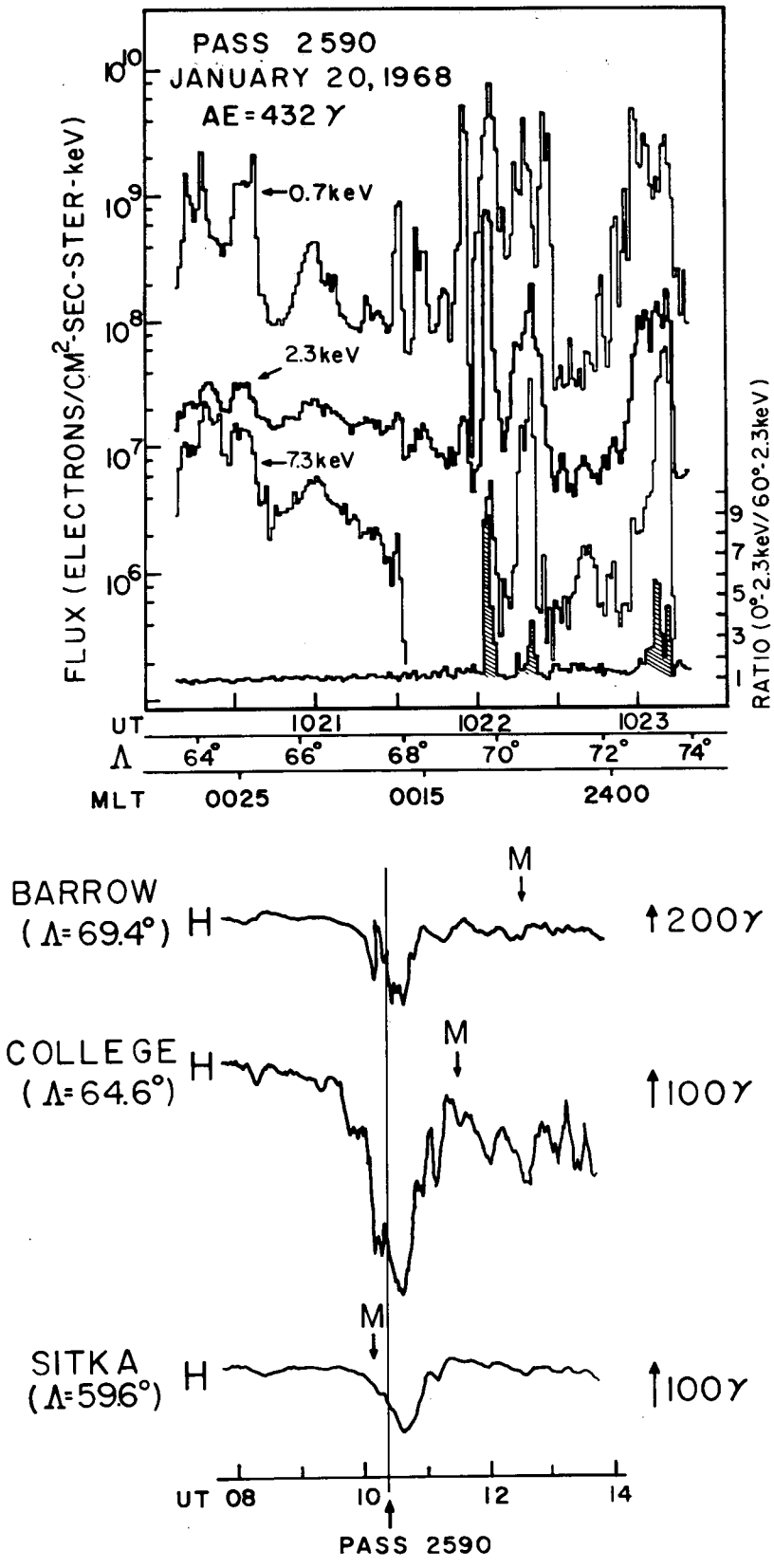
PASS 2590
JANUARY 20, 1968
AE = 432 γ
0.7keV
2.3keV
7.3keV
FLUX (ELECTRONS/CM²-SEC-STER-keV)
RATIO (0°-2.3keV/60°-2.3keV)
UT
1021
1022
1023
Λ
64°
66°
68°
70°
72°
74°
MLT
0025
0015
2400
BARROW
(Λ=69.4°)
H
M
200γ
COLLEGE
(Λ=64.6°)
100γ
SITKA
(Λ=59.6°)
UT 08
10
12
14
PASS 2590

Figure 11

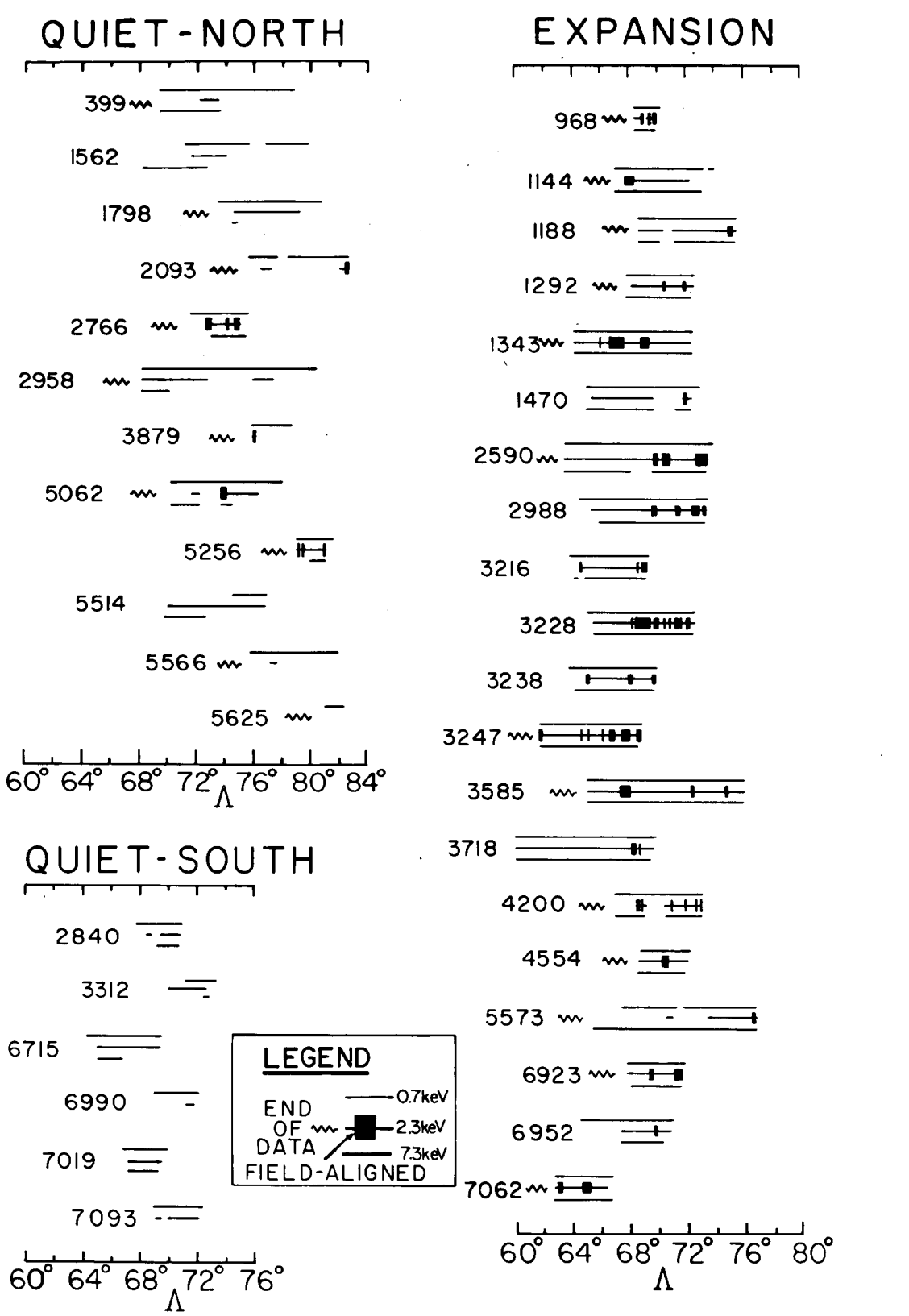
QUIET-NORTH
399
1562
1798
2093
2766
2958
3879
5062
5256
5514
5566
5625
60° 64° 68° 72° 76° 80° 84°
Λ
QUIET-SOUTH
2840
3312
6715
6990
7019
7093
60° 64° 68° 72° 76°
Λ
LEGEND
END OF DATA
FIELD-ALIGNED
0.7keV
2.3keV
7.3keV
EXPANSION
968
1144
1188
1292
1343
1470
2590
2988
3216
3228
3238
3247
3585
3718
4200
4554
5573
6923
6952
7062
60° 64° 68° 72° 76° 80°
Λ
NASA-GSFC

Figure 12